Institute of Space and Aeronautical Science, University of Tokyo
Report No. 426, July 1968

Rocket-Borne $dE/dx \cdot E$ Semiconductor Detector Telescope for Particle Identification*

By

Tadayoshi DOKE**, Katsuaki NAGATA***, Shigeo NAKAGAWA***
Akira SASAKI**** and Masahiro TSUKUDA***

Summary: Basic considerations on a particle identification method utilizing $dE/dx \cdot E$ products, including a discussion on the limitation of isotope separation for heavy charged particles, are described and a geometrical design of $dE/dx \cdot E$ counter telescope is presented. Based on these considerations, rocket borne instruments capable of observing the abundance ratio of protons, deuterons and tritons in the Van Allen belt were constructed. The system performance, the characteristics of the silicon dE/dx detectors, and the results of the rocket experiments are briefly described.

1. INTRODUCTION

Identification of charged particles by simultaneous determinations of the rate of energy loss dE/dx and the total energy E_0 has been widely used in low energy nuclear reaction experiments, in which proportional counters or pulse ionization chambers are frequently selected as dE/dx counters. For high energy particles, however, gas counters are not suitable because of the low rate of energy loss. Thin scintillation counters show high rate of energy loss but suffer from the poor light collection efficiency, non linearity of light out-put with particle energy and dependence of light out-put on types of particles. Recently semiconductor detectors have become widely used because of their compactness, improved energy resolution and good linearity of ionization yield with particle energy. We tried to use semiconductor $dE/dx \cdot E$ telescope for identification of protons, deuterons and tritons in the Van Allen belt and heavy charged particles including C-12, C-13 etc. in the primary cosmic rays.

In this paper we will first give a basic consideration for particle identification over broad energy range and discuss limitations of isotope identification in heavy charged particles. Next we will describe general design principles of the detector telescope including the characteristic of the transmission type detectors and elec-

* A part of the Research Project of Space Science of the Institute of Space and Aeronautical Science.
** Institute for Nuclear Study, University of Tokyo, Tanashi-shi, Tokyo, Japan.
*** Department of Physics, Rikkyo University, Ikebukuro, Tokyo, Japan.
**** Institute for Atomic Energy, Rikkyo University, Tokyo, Japan.

tronic circuits. Finally we will give the system performance and the results of rocket observations on the abundance ratio of protons, deuterons and tritons in the Van Allen belt.

2. Particle Identification Method

To a first approximation, in the non-relativistic case, the energy lost by a particle in traversing a given thin layer of absorber is proportional to Mz^2/E_0, where M is the particle mass, z its charge and E_0 its energy. If a particle first traverses a thin dE/dx detector and is afterwards stopped in a thick E detector, and if the signal in both detectors is linear with energy absorbed, then the product of the two signals is a measure of the quantity Mz^2. A $dE/dx \cdot E$ detector is an assembly of two counters in line and pulse height multiplication is done electronically. Measurement, by this method, of a quantity roughly proportional to Mz^2 is very useful for particle identification, as the expression takes the values 1, 2, 3, 12 and 16 for protons, deuterons, tritons, ^{3}He and alphas, respectively.

i) Correction Factor for $dE/dx \cdot E$ Function

A detailed examination of the processes which result in improper identification signals indicates that the following correction factors should be involved.

a) The general formula for the rate of energy loss is given as [1]

$$\frac{dE}{dx} = \frac{4\pi e^4 z^2}{mv^2} \cdot N \cdot Z \cdot \left\{ \ln \frac{2mv^2}{I} - \ln(1-\beta^2) - \beta^2 \right\} \qquad (1)$$

where

e, m = charge and mass of the electron
Z = atomic number of the absorber
β = particle velocity/velocity of light
v = velocity of incident particle
N = number of atoms per cc of the absorber
I = average energy to ionize and excite atoms of the absorber

Because of the variation of the logarithmic terms with energy, the product $(dE/dx)_{E=E_0} \cdot E_0$ is not a constant but decreases at low energies as shown in Fig. 1 (a). To partially correct for this, it has become common to calcutate $(dE/dx)_{E=E_0} \cdot (E_0 + E')$, where E' is an adjustable constant. Since dE/dx becomes small at high energies, addition of $(dE/dx)_{E=E_0} \cdot E'$ makes the product $(dE/dx)_{E=E_0} \cdot (E_0 + E')$ almost constant over a wide energy range.

b) We have assumed that the thin transmission type detector absorbs only a very small fraction of the total particle energy and the energy deposited in the detector can be regarded as $(dE/dx)_{E=E_0}$. In practice, however, the rate of energy loss changes gradually as the particle traverses the detector. To correct for this factor we should regard the particle as having total energy of $(E + k\Delta E)$, where E and ΔE are energy deposited in E and dE/dx counters and k is an adjustable constant. If ΔE is small compared with E_0, the correct value for k is 0.5, because

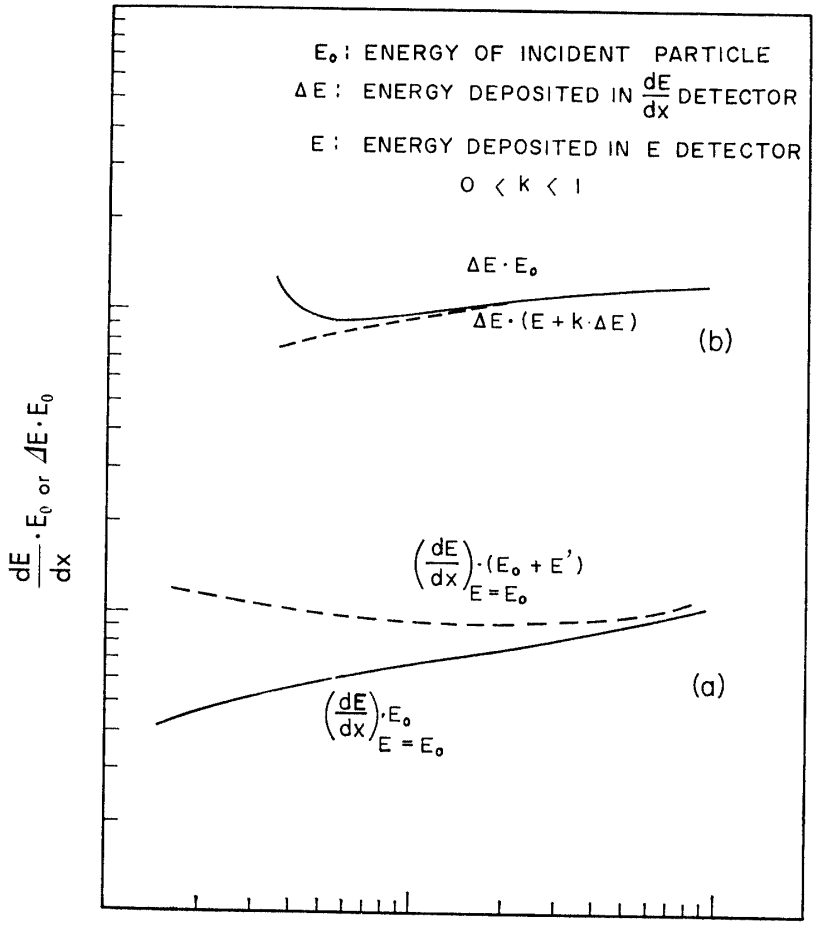

FIG. 1. (a) Effect of the logarithmic term in Eq. (1).
(b) Thickness effect of dE/dx detector.

$E+0.5\Delta E$ can be considered as a measure of the average energy in the region over which ΔE can be regarded as dE/dx. Also, k should be less than 1, because ΔE which is proportional to a mean rate of energy loss in the transmission type detector, is larger than that expected for a incident particle of energy E_0. In general, k lies between 0 and 1. In spite of the introduction of the adjustable constant k, however, it is obviously impossible to regard ΔE as determining the rate of energy loss over a broad energy range. Fig. 1(b) shows a typical curve of the product of $\Delta E \cdot E_0$ versus E_0 for a transmission type detector with finite thickness and a curve corrected by using the adjustable constant k. In general, the quantity $\Delta E(E+E'+k\Delta E)$ has been widely used as a useful measure for particle identification over wide energy range and the constant k and E' are adjusted to obtain the best results in a given experiment. Fig. 2(a), (b) and (c) show the variation of the product of ΔE and $E+E'+k\Delta E$ with the energy of incident particle for proton, deuteron and triton adjusted so that the product be constant for the various thickness of the detector.

ii) Resolution for Particle Identification

The resolution or the spread of the pulse height distribution of the product pulses must be sufficiently small so that adjacent isotopes can be easily separated.

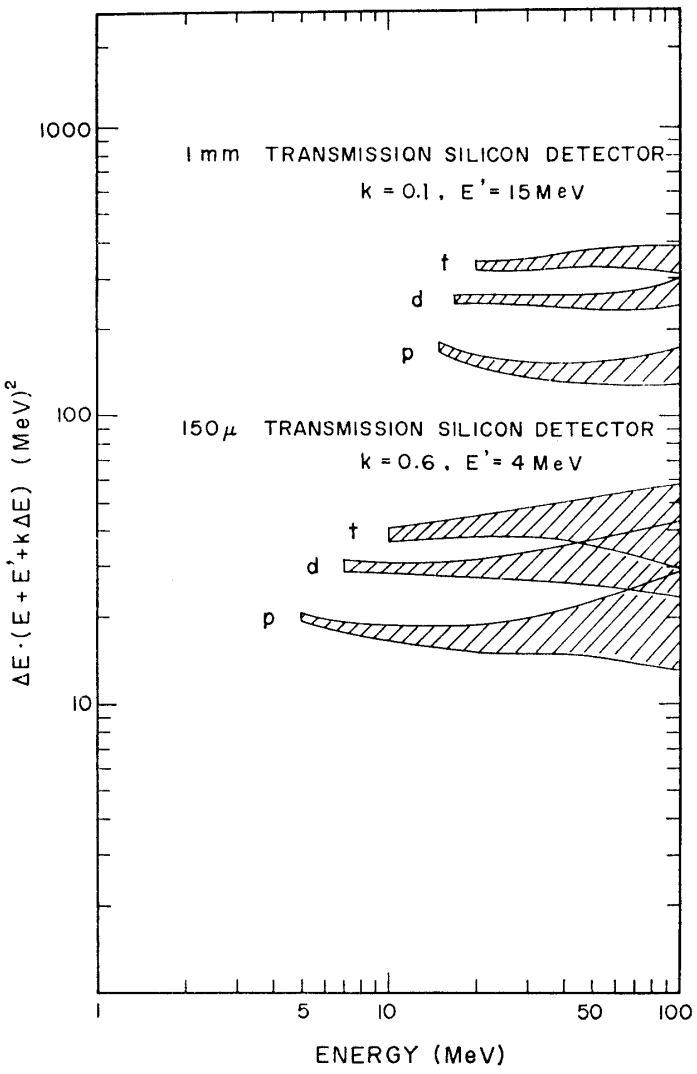

FIG. 2. (a) (b)

FIG. 2. Variation of the product of ΔE and $E+E'+k\Delta E$, adjusted as the product be constant for proton, deuteron and triton, with particle energy for dE/dx detector 150 μ thick (a), 1,000 μ (b) and 500 μ (c). Shaded areas show statistical spreads expressed by full width at half maximum.

This spread results from the following causes; (a) statistical fluctuation in energy loss in the transmission detector, (b) electronic circuit noise, (c) the variation of energy loss due to oblique incident particles. As will be described later, the contribution from the electronic noise is smaller than the statistical effect and the contribution from (c) can be reduced by the selection of solid angle of the telescope. The statistics of the energy loss of a charged particle traversing a thin material were calculated by Landau [2], Symon [3] and Vavilov [4].

As a criterion in the statistics, we have the following dimensionless parameter [4], [5].

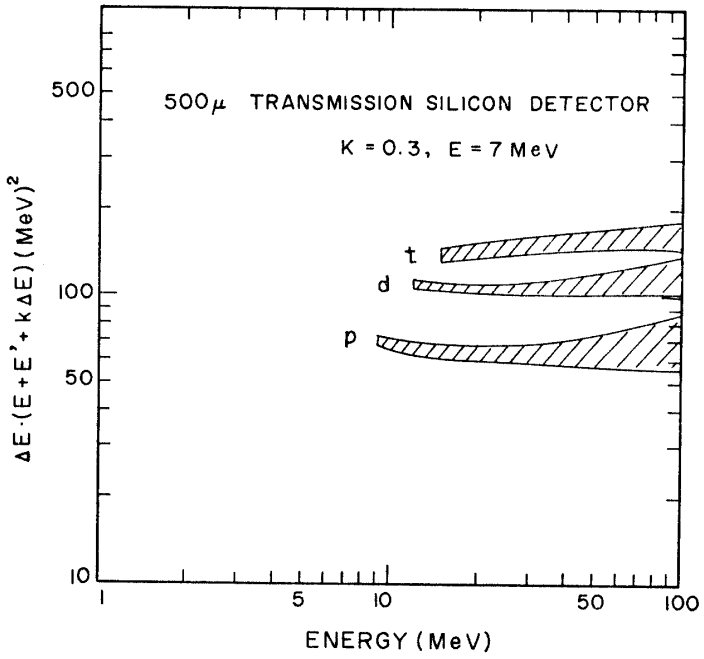

FIG. 2. (c)

$$K=\frac{2\pi e^4N}{mv^2}\cdot z^2\cdot\rho\cdot\frac{Z}{A}\cdot\frac{x}{E_{\max}}=\frac{W}{E_{\max}}\qquad\left(W=\frac{2\pi e^4N}{mv^2}\cdot z^2\cdot\rho\cdot\frac{Z}{A}\cdot x\right)\qquad(2)$$

where ρ, x and A are the density, thickness and mass number of absorbing material and $E_{\max}$ the maximum energy of scattered electron. For $K\gg1$, the fluctuation of the energy loss shows the Gaussian distribution, while for $K\ll1$, the fluctuation shows the Landau distribution. In both cases, the r.m.s deviation in the energy loss are approximately given as follows [5];

for Gaussian distribution $\qquad\sigma_g=W^{1/2}\cdot E_{\max}^{1/2}\qquad(3)$

for Landau distribution $\qquad\sigma_l=2W\qquad(4)$

In Fig. 2, the shaded parts along the curves show the statistical spreads expressed by full width at half maximum, which were estimated from the formula (3) and (4). As shown in this figure, the shaded areas for proton, deuteron and triton overlap each other in the high energy region. Since K increases with the thickness of the transmission type detector, the limitation of particle identification caused by such overlaps of statistical spreads can be improved by the use of thicker detector

Now, let us consider about the separation of a very heavy particle from adjacent isotopes. The following quantity should serve as a good measure in isotope separation.

$$R=\text{statistical spread of }(dE/dx\cdot E_0)_{M,z}/\{(dE/dx\cdot E_0)_{M+1,z}-(dE/dx\cdot E_0)_{M,z}\}$$

Using the formula (3) and (4), R is written as follows,

for Gaussian distribution in $K\gg1$

$$R_g=\frac{(E_0\cdot dE/dx)_{M,z}\cdot\dfrac{E_{\max}^{1/2}\cdot W^{1/2}}{(dE/dx)_{M,z}\cdot x}}{\Delta(E_0\cdot dE/dx)_{M,z}}=\frac{E_0\cdot E_{\max}^{1/2}\cdot W^{1/2}}{\kappa(\beta)z^2x}$$

$$\sim\frac{1}{\kappa(\beta)\sqrt{x}}\frac{E_0}{z} \qquad (5)$$

$$\left(\text{assuming that } E_{\max}=4\frac{m}{M}E_0\right)$$

for Landau dustribution in $K\ll 1$

$$R_l=\frac{(E_0\cdot dE/dx)_{M,z}\cdot\dfrac{E_{\max}^{1/2}\cdot W^{1/2}}{(dE/dx)_{M,z}\cdot x}}{\Delta(E_0\cdot dE/dx)_{M,z}}=\frac{2E_0\cdot W}{\kappa(\beta)\cdot z^2\cdot x}\frac{E_0}{\beta^2\kappa(\beta)} \qquad (6)$$

where $\kappa(\beta)$ is given by $\Delta(E_0\cdot dE/dx)_{M,z}=\kappa(\beta)\cdot z^2$ and x is thickness of detector. Since z is proportional to M and κ depends only on the velocity of incident particle, the non-relativistic approximation in the formula (5) shows that a dE/dx•E detector telescope has the same resolution for particles with the same energy per nucleon. In other words, if the energy per nucleon of incident particle is constant, the ability of the telescope for particle identification between two adjacent isotopes does not depend on the particle mass M. Accordingly, if the identification for adjacent isotopes with small mass number such as protons or alpha-particles can be achieved, it may be done as well for those with large mass number. From the formula (5), it is obvious that the resolution deteriorates with increase of particle energy and the statistical fluctuation gradually develops into the Landau type. In the region of the Landau statistics, generally, the mass idenification due to this method is difficult even for light particles as previously shown in Fig. 2.

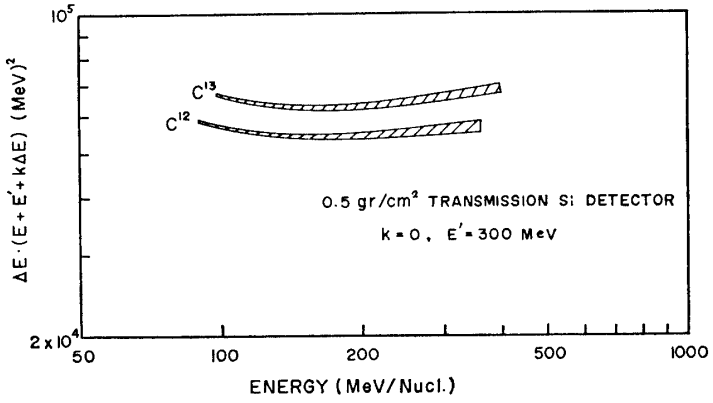

FIG. 3. Variation of the product of ΔE and $E+E'+k\Delta E$, adjusted as the product be constant over broad energy range near 100 MeV/nucleon for C-12 and C-13, with particle energy for dE/dx detector 500 μ thick. Shaded areas show statistical spreads expressed by full width at half maximum.

As a measure of energy per nucleon of incident particle in the transition from the Gaussian to the Landau fluctuation, we have a quantity $W/4$m. In the non-

relativistic region, the condition for the Gaussian fluctuation of energy loss is expressed by $E_0/M \ll W/4\text{m}$, while for Landau's fluctuation $E_0/M \gg W/4\text{m}$. Since W is proportional to z^2, these conditions show that the transition from the Gaussian to the Landau fluctuation for particles with high z occurs in higher energy region than that for particles with low z. Accordingly, we can conclude that, if the condition for the Gaussian fluctuation is satisfied, the mass identification for heavy particles can be more easily achieved than for light particles.

For example, let us consider about identification between C-12 and C-13. In a transmission type silicon detector of 0.5 g/cm^2 thick, E_0/M as the criterion of transition of the statistics, is 440 MeV/nucleon.* Accordingly, in the energy region near 100 MeV/nucleon, the fluctuation of energy loss is the Gaussian type.

Using the formula (5), the full width at half maximum (fwhm) of pulse height distribution for the energy loss in the dE/dx detector is estimated to be about 3.5% at 100 MeV/nucleon. Since the difference between both $dE/dx \cdot E$ functions of C-12 and C-13 is 8%, the separation between these isotopes can be almost completely achieved by $dE/dx \cdot E$ detector telescope. Fig. 3 shows the $dE/dx \cdot E$ functions of C-12 and C-13, (which are adjusted so as to have constant values respectively in the energy region near 100 MeV/nucleon), with statistical spreads for dE/dx silicon detector of 0.5 g/cm^2 thick. Since, at present, it is not easy to fabricate silicon detector thicker than 3 mm, we plan to construct a E-detector system composed of four or five transmission type silicon detectors stacked in series and electrically connected in parallel.

3. Design of $dE/dx \cdot E$ Detector Telescope

In the design of $dE/dx \cdot E$ detector system, the geometry of detector arrangement and thickness of dE/dx detector are important factors in order to satisfy such requirements as a large detectable solid angle and the use over a broad energy range.

The distribution of deposited energy in the dE/dx detector caused by different incident angles is shown in Fig. 4 for various ratios of L/D, where L is a distance between dE/dx and E detector and D is a diameter of the detector (See Appendix). The geometry of the detector system should be designed so that the spread may be negligibly small compared to statistical spread and noise broadening. The thickness of dE/dx detector should be selected considering measurable energy range. As we have used surface barrier silicon detectors 150 to 200 μ thick as dE/dx-counters and a Li-drift type silicon detector 2700 μ thick as E-counter, the useful range for particle identification for proton is from 5 MeV to 30 MeV. The statistical fluctuation (fwhm) of $dE/dx \cdot E$ signal is about 30% in the high energy range and 8% in the low energy region. To keep the variation of energy loss in dE/dx-counter due to oblique incident particles less than 2%, small compared with the statistical flucuation in the dE/dx-counter, the ratio L/D should be

* This value is obtained from the condition of $K=\frac{W}{E_{\max}}=1$ and the approximate fomula $E_{\max}\approx\frac{2\beta^2}{1-\beta^2}mc^2$.

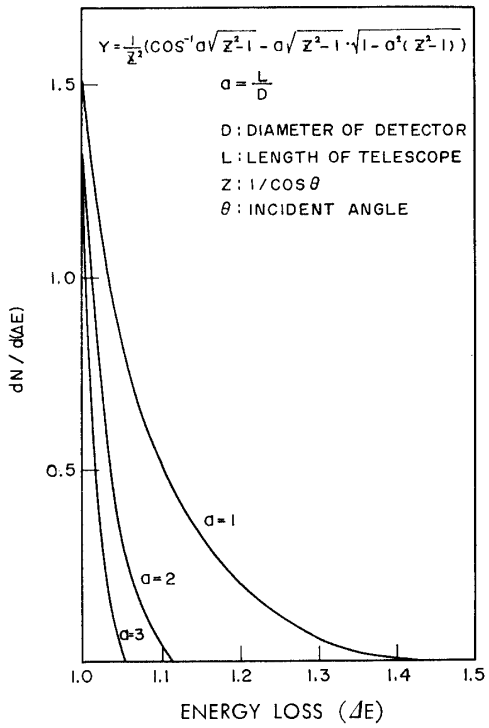

FIG. 4. Distribution of deposited energy in dE/dx detector due to oblique incident particles for different telescope geometries, which are given by ratio of distance L between dE/dx and E detectors to the detector diameter D.

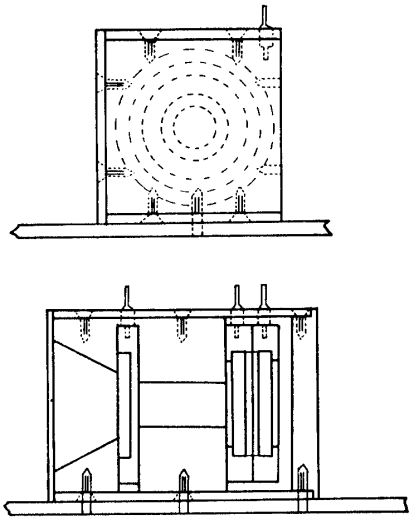

FIG. 5. A cross sectional view of $dE/dx \cdot E$ telescope counters.

at least 2.

Fig. 5 shows a cross sectional view of the telescope counter. The third detector was used in anticoincidence mode in order to remove traversing particles through the E detector. The effective solid angle is about 0.66 steradian. The side wall was made of Al, which has small cross section for protons of energy larger than 100 MeV. Assuming the cross section to be 5×10^{-26} cm^2 [6], the background counting rate originating from the nuclear reaction in Al by protons in the Van Allen belt is estimated to be of the order of 10^{-6} to one proton flux, which may be completely ignored.

4. Instruments Assembly and Electronic System

Based on the design principle given above, three rocket borne instruments were built. Each instrument is specifically designed for compactness, light weight, and low power consumption. It consists of two containers, one housing the detectors and pre-amplifiers and the other the associated electronics including analog pulse multiplier. The instrument weighs 3.5 Kg. Power consumption is 2.5 watts at 12.5 volt D.C.. Fig. 6 is a photograph of the complete assembly. The entire system has undergone an environmental test in order to qualify it for the rigors of launch and flight.

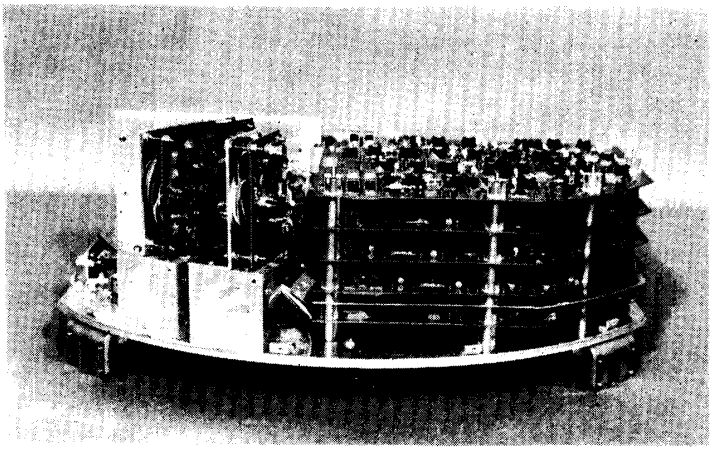

FIG. 6. Photograph of the rocket borne instrument.

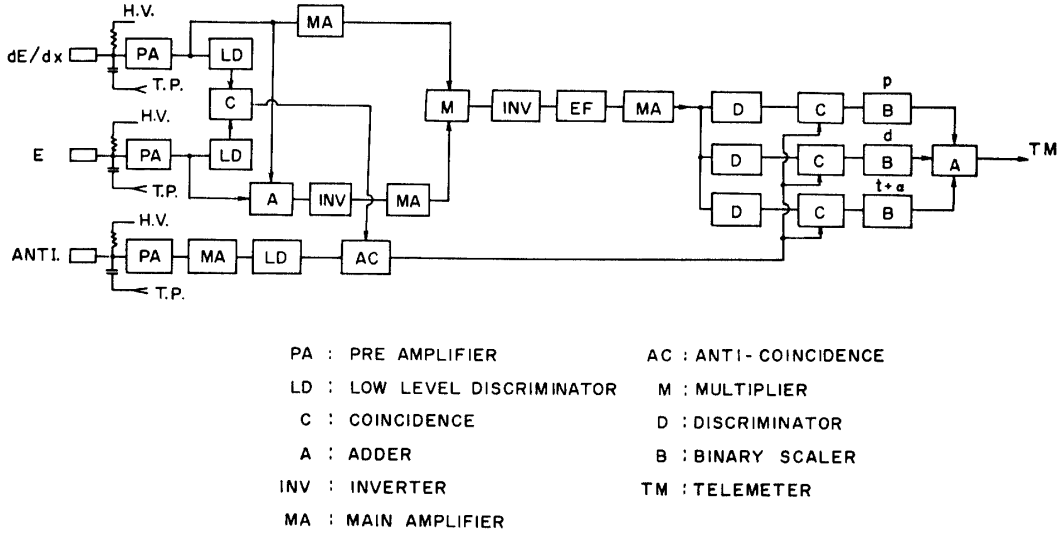

FIG. 7. Block diagram of the electronic system.

Fig. 7 gives the block diagram of the electronic system. The voltage pulses from dE/dx and E charge sensitive pre-amplifiers are applied to an analog multiplier circuit. The resultant output pulse of the form $\Delta E(E+E'+k\Delta E)$ which is nearly proportional to Mz^2 is analyzed by a stacked discriminator type 3 channel pulse height analyzer. The threshold levels of the discriminators are so adjusted that the pulse heights corresponding to the 1st channel represents protons, the 2nd channel deuterons, and the 3rd channel tritons and particles heavier than tritons. The number of counts in each channel is telemetered to grounds. The multiplier circuit is based on the principle originally introduced by Swenson [7]. Fig. 8 shows the circuit diagram. Only six switching transistors are used. The measured circuit characteristics are given in Fig. 9 in which the ordinate is multiplier output voltage V_{out}, the abscissa is ΔE and the parameter is E. From these characteristics V_{out} is seen to be proportional to the product $(E+E')(\Delta E+\Delta E')$. By adjusting the gain of the amplifiers for E and ΔE signals we can make E' equal to 4 MeV and $\Delta E'$ nearly equal to zero. As described previously the actual product should be

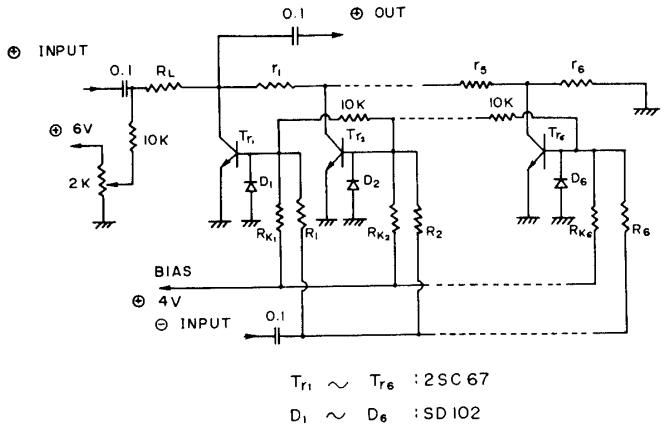

FIG. 8. Multiplier circuit diagram.

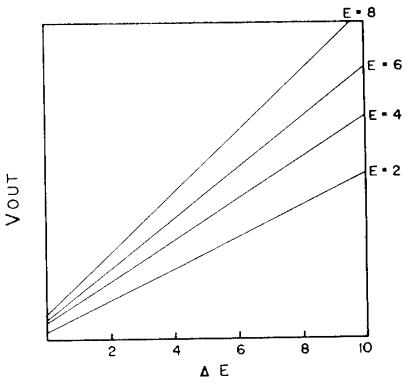

FIG. 9. Measured characteristic of the multiplier circuit.

$\Delta E \cdot (E + E' + k\Delta E)$, so that we used $E + k\Delta E$ instead of E as shown in the block diagram in the Fig. 7. Examples of the expected output voltage ratios of deuteron/proton and triton/proton for 12 MeV particles passing through 160 μ thick (dE/dx) detector and stopped in the E detector are estimated to be 1.43 and 1.83 respectively.

5. TRANSMISSION TYPE SILICON DETECTOR

In the $dE/dx \cdot E$ semiconductor detector system, not only dE/dx detector but also E-detector must be a transmission type, because particles traversing E detector must be eliminated in anticoincidence with signals from the third detector put behind the E-detector.

i) Surface Barrier Transmission Detector

From N-type silicon wafer of 20 mm in diameter, 250 μ thick and specific resistivity of 850 Ω-cm, a disk 150 to 200 μ thick with uniformity of $\pm 2\%$ was

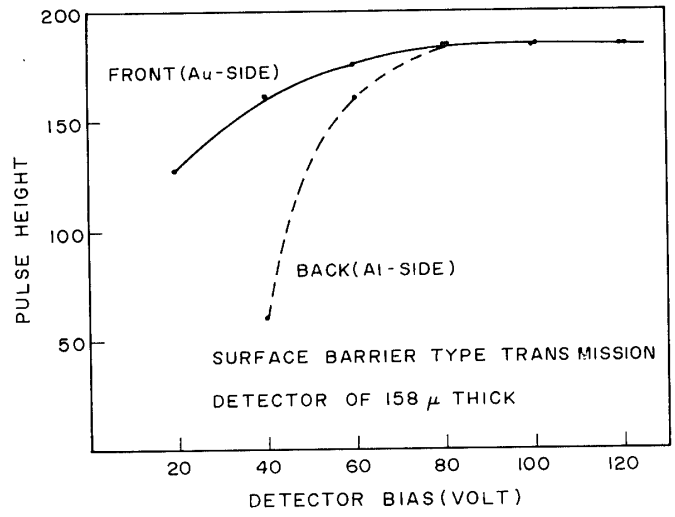

FIG. 10 (a)

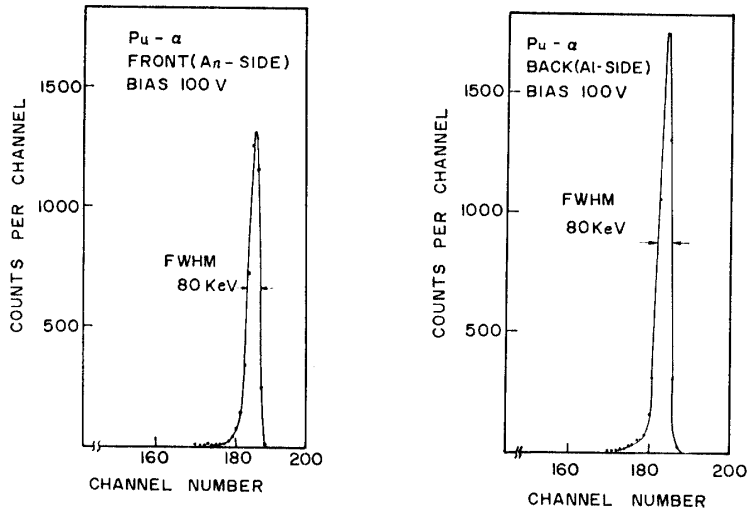

(b)

FIG. 10. Characteristics of surface barrier type *dE/dx* detector for Pu-239 alpha-particles incident upon the "front" and "back" surface. (a) saturation curves of pulse height versus applied voltage and (b) pulse height distributions.

fabricated by polishing and chemically etching. The "front surface" of the silicon disk was coated by evaporated Au film of 50 to 100 $\mu g/cm^2$ thick and the "back surface" by Al film of 100 $\mu g/cm^2$ thick. The sensitive area is 1.13 cm^2 (12 mm in diameter). Fig. 10(a) shows the saturation curves of peak pulse height versus applied voltage for Pu-239 alpha-particles incident upon the "front" and "back" surface, and Fig. 10(b) shows their pulse height distributions.

ii) Li-drifted Transmission Detector

The so-called Li-drifted surface barrier silicion detector [8], [9] was fabricated from P-type silicon wafer of 20.5 mm in diameter, 3 mm thick and specific resistivity of 700 Ω-cm. After P-type impurities over a whole region were compensated by

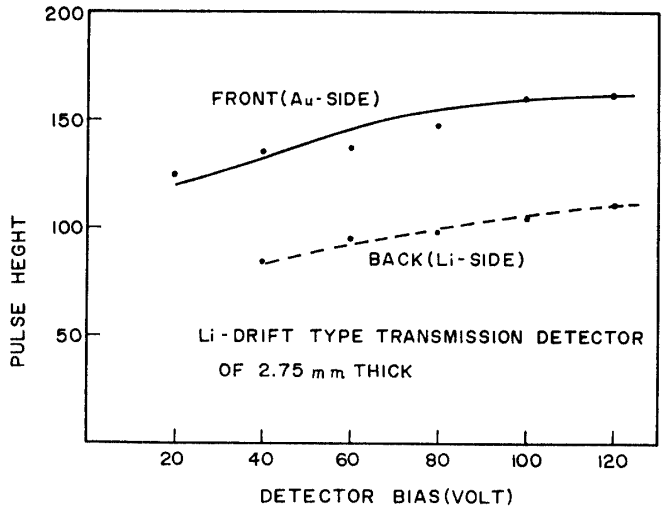

FIG. 11 (a)

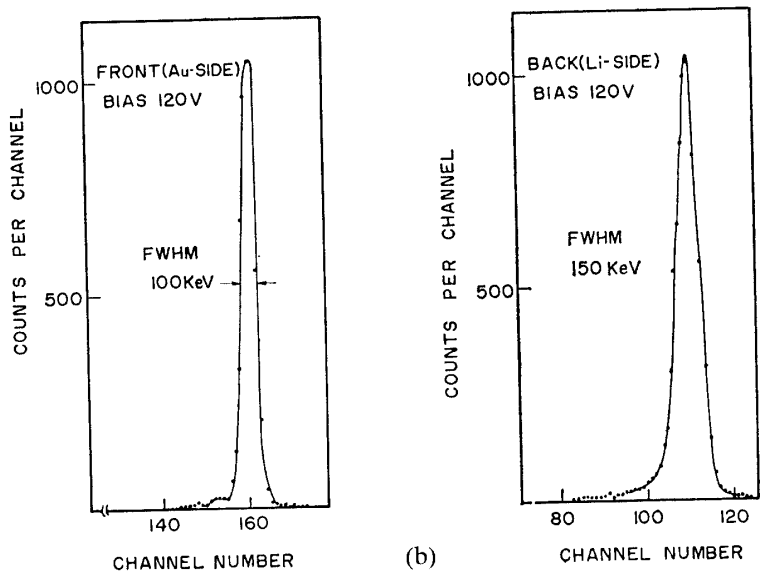

FIG. 11. Characteristics of Li-drift type dE/dx detector for Pu-239 alpha particles incident upon the "front" and "back" surface.
(a) saturation curves of pulse height versus applied voltage, and
(b) pulse height distributions.

Li ions, thick Li layer initially coated was removed by polishing process, and the thickness (2.7 mm) of the silicon disk was adjusted so as its uniformity is within $\pm 2\%$ by polishing and chemically etching. Then Au film of 50 to 100 $\mu g/cm^2$ thick was evaporated on the initially Li coated side and Al film of 100 $\mu g/cm^2$ thick on the reverse side. Fig. 11(a) shows the saturation curves of pulse height with applied voltage for detector having sensitive region of 1.5 cm^2, and Fig. 11(b) shows the pulse height distributions. In both type detectors, the full width at half maximum of pulse height distribution for Pu-239 alpha-particles is about 100 KeV.

6. System Performance

The $dE/dx \cdot E$ detector system was exposed to mixed particle flux for the test of the system performance. Fig. 12 and Fig. 13 show a spectrum of $dE/dx \cdot E$ pulses due to recoil protons and deuterons emitted from a frozen heavy water target and that due to reaction protons, deuterons and tritons from a thin Li target when bombarded by 14 MeV neutrons. From Fig. 12, it can be seen that the separation between recoil deuteron pulses and recoil proton pulses are wide enough to discriminate recoil deutrons from recoil protons, even when the intensity ratio is less than 1:1000. The observed peak value ratio of identifier pulse heights is 1.37 for deuteron/proton and 1.73 for triton/proton, which may be compared with the calculated value of 1.43 and 1.83.

7. Rocket Experiment

We have carried out three rocket experiments to measure hydrogen isotope abundance in the Van Allen belt. L-3H type sounding rockets were launched from

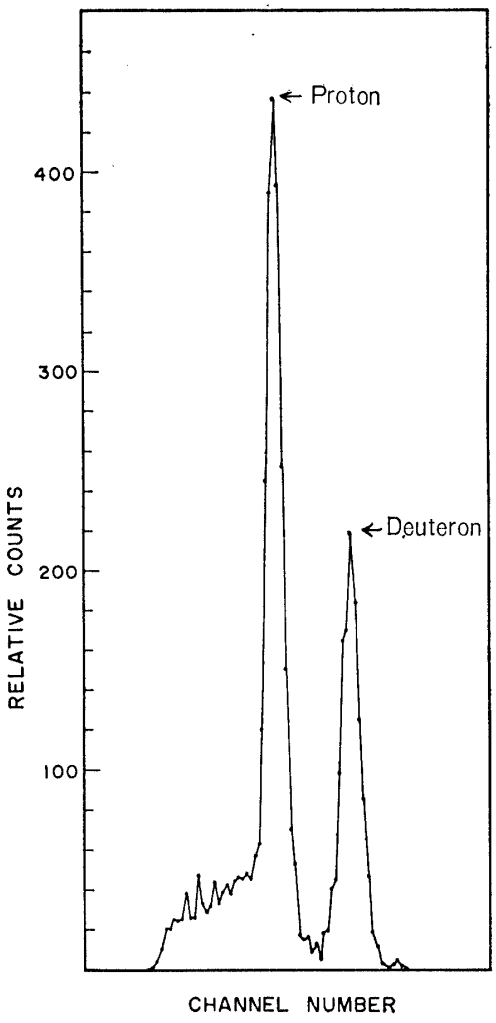

FIG. 12. Spectrum of $dE/dx \cdot E$ pulses due to recoil protons and deuterons emitted from a frozen heavy water target bombarded by 14 MeV neutrons.

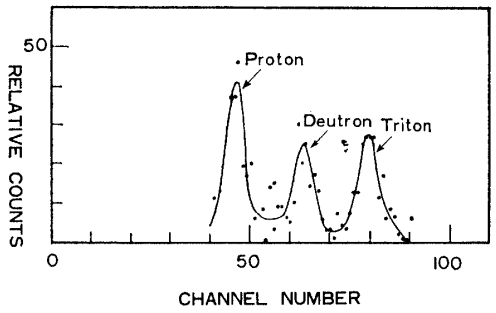

FIG. 13. Spectrum of $dE/dx \cdot E$ pulses due to reaction protons, deuterons and tritons emitted from a thin Li target bombarded by 14 MeV neutrons.

the Kagoshima Space Center (131° 05′E, 31°15′N) in charge of the Institute of Space and Aeronautical Science, University of Tokyo, during the period from March 1966 to February 1967. The L-3H-2 rocket which was launched with an initial elevation angle of 78°, to the azimuth of 85° from the north was successful and attained a maximum altitude of 1,800 Km. All the electronic instrument performed their function perfectly. Fig. 14 shows the variation of proton counting rate with flight time of the rocket. The marked increase in the counting rate

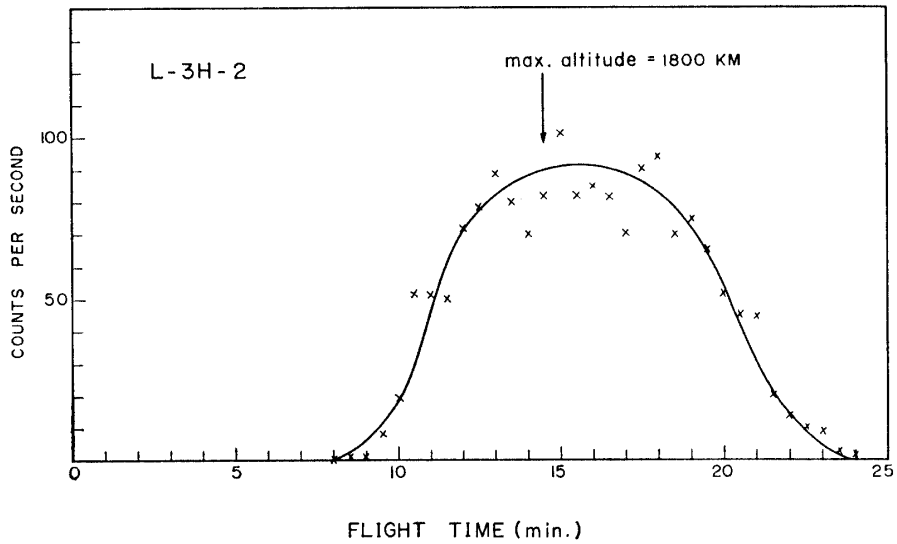

FIG. 14 Variation of proton counting rate with flight time of L-3H-2 rocket.

about 8 minutes after the launch of the rocket clearly shows the beginning of the Van Allen belt. The rate rapidly reached its maximum value at the time 12 minutes and remained rather constant until the time 18 minues when it again began to decrease, while the rocket reached the maximum altitude of 1,800 Km at the time 14 minutes 45 seconds. The total counts of protons during the entire flight was estimated to be 48,000, while that of deuterons only 4 and that of tritons and heavier particles 6. The abundance ratio for deuteron/proton and triton/proton in the Van Allen belt is estimated, with some statistical uncertainty, to be 0.8×10^{-4} and 1.2×10^{-4} respectively.

Appendix: Energy Loss Distribution due to Oblique Incidence Particles

Fig. A-1 shows schematically a geometry of detector arrangement in a typical $dE/dx\cdot E$ detector system. When a parallel beam of particles enters into the

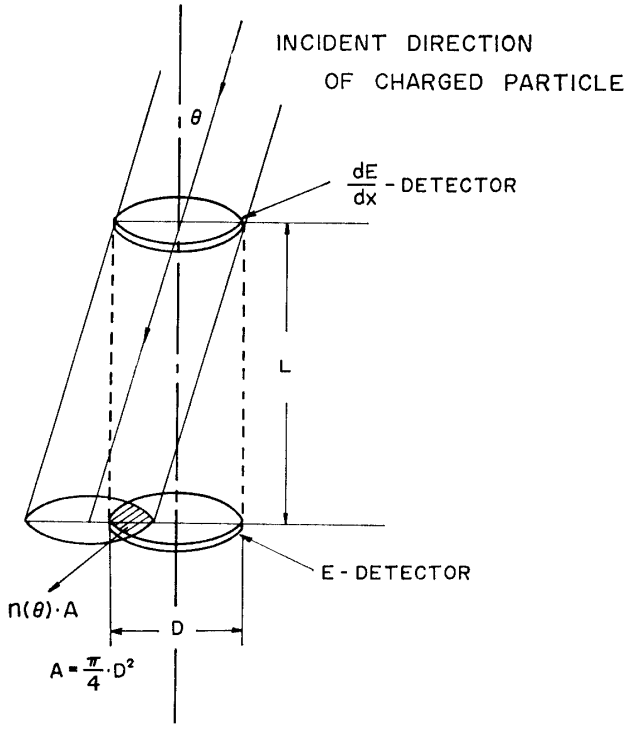

Fig. A–1. Typical geometry of detector arrangement in $dE/dx\cdot E$ telescope.

$dE/dx\cdot$detector at incident angle θ, the rate of the beam flux traversing both detectors of dE/dx and E is proportional to a shaded area in the figure. If the direction of the incident particle is isotropic, the number of particles, which traverse the dE/dx-detector and enter into the E-detector at an angle between θ and $\theta+d\theta$, is

$$dN=\phi\cdot\eta(\theta)\cdot A\cdot\cos\theta\cdot\frac{\sin\cdot\theta\, d\theta}{2} \tag{A-1}$$

where ϕ is the flux of incident particle, A the area of the detectors and $\eta(\theta)$ is ratio of the area of the shaded region in Fig. 1-A to A. The energy loss of the particle entering into the dE/dx-detector at an angle θ is

$$\Delta E_\theta=\frac{\Delta E_n}{\cos\theta} \tag{A-2}$$

where ΔE_n is the energy loss for the normal incident particle.

From (A-1) and (A-2), we have

$$\begin{aligned}\frac{dN}{d(\Delta E_\theta)}&=\frac{1}{2}\cdot\phi\cdot A\cdot\frac{D^2}{2}\cdot\{\cos^{-1}a\sqrt{x^2-1}-a\sqrt{x^2-1}\sqrt{1-a^2(x^2-1)}\}/x^3\\&=\frac{1}{2}\cdot\phi\cdot A\cdot\frac{D^2}{2}\cdot Y\end{aligned} \tag{A-3}$$

where $x=\dfrac{1}{\cos\theta}$, $a=\dfrac{L}{D}$, $Y=\{\cos^{-1}a\sqrt{x^2-1}-a\sqrt{x^2-1}\sqrt{1-a^2(x^2-1)}\}/x^3$, and D is a diameter of detector and L a distance between dE/dx and E detectors. Fig. 4 shows the Y distribution obtained from the equation (A-3).

References

[1] Bethe, H. A. and Ashkin, J.: "Passage of Radiations through Matter", Part II in "Experimental Nuclear Physics" edited by E. Segre, John Wiley & Sons, Inc., New York, Chapman & Hall, Limited, London (1953).

[2] Landau, L.: "On the Energy Loss of Fast Particle by Ionizations", J. Phys. USSR Vol. 8, (1944) p. 201.

[3] Rossi, B.: "Theory of Electromagnetic Interactions", Chapter 2 in "High Energy Particles", Prentice-Hall, Incorporated, New York (1952).

[4] Vavilov, P. V.: "Ionization Losses of High-Energy Particles", Soviet Physics JETP, Vol. 5, (1957) p. 749.

[5] Ritson, D. M.: "General Properties of Particles and Radiation", Chapter 1 in "Techniques of High Energy Physics" edited by D. M. Ritson, Interscience Publishers, Inc., New York (1961).

[6] Friedlander, G., Hudis, J. and Wolfgang, R. L.: "Disintegration of Aluminum by Protons in the Energy Range 0.4 to 3.0 BeV", Phys. Rev., Vol. 99, (1955) p. 263.

[7] Swenson, L. W.: "A Charged Particle Identification System with Broad Energy Range" Nucl. Instr. and Method, Vol. 31, (1964) p. 269.

[8] Bertolini, G., Cappellani, F. and Restelli, G.: "Construction and Performances of Silicon Lithium Drifted Detectors", Nucl. Instr. and Method, Vol. 32 ,(1965) p. 86.

[9] Murray, H. M., Harpster, J. W. and Casper, K. J.: "Fabrication Methods for Lithium Drifted Surface Barrier Silicon Detectors", Nucl. Instr. and Method, Vol. 40 (1966) p. 330.